Published in the Slovak Republic
Nanotechnology Research and Practice
Has been issued since 2014.
E-ISSN: 2413-7227
2019, 6(1): 3-9

DOI: 10.13187/nrp.2019.6.3
www.ejournal13.com

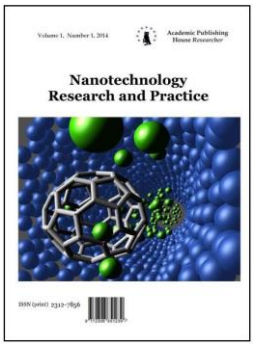

Indazole, Pyrrole and 2-Pyrone Compounds as Corrosion Inhibitors for Mild Steel in Acidic Medium: DFT Analysis

M. El idrissi [a, *], S. Zouitina [a], A. Barhoumi [b], A. Zeroual [b], A. Tounsi [a], K. El Harfi [a], M. Mbarki [a]

[a] Sultan Moulay Slimane University, Faculty Polydisciplinary, Beni-Mellal, Morocco
[b] Chouaïb Doukkali University, Faculty of Science, El Jadida, Morocco

Abstract

In the present work we used density functional theory (DFT) with B3LYP/6-31G to study the reaction 6-Methyl-3-[1-(2-methyl-2H-indazol-6-ylamino)-ethylidene]-pyran-2,4-dione (R1), 3-[1-(2-Allyl-2H-indazol-6-ylamino)-ethylidene]-6-methyl-pyran-2,4-dione (R2) and 6-(2,5-Dimethyl-pyrrol-1-yl)-2-ethyl-2H-indazole (R3) were synthesized and examined as corrosion inhibitors for mild steel in 1.0 M HCl. It is noticed that R1 as more effective inhibitor than R3, this last as more effective inhibitor than R2. The theoretical calculation validate that these compounds can suck up on the mild steel surface by distributing the separate pair electrons of the hetero-atoms with iron atoms or by admitting electrons from the iron surfaces. The presence of the pyrrole group is assumed to be responsible for the elevated inhibition efficiency of R1. Determining the energies of the frontier molecular orbitals, chemical potentials, transfer charge quantities, and electrophilicity and nucleophilicity indices. We used the same method to calculate ionisation potentials, electronic affinities, hardness, softness, electrophilic Parr functions and the nucleophilic Parr.

Keywords: corrosion inhibitor, mild stee, DFT, electrophilic Parr, nucleophilic Parr, indazol.

1. Introduction

The investigation of corrosion inhibition of mild steel via organic inhibitors typically in acidic media is one of the most essential themes of modern study in diverse industries (van der Geer et al., 2010; Singh et al., 2014; Chafaa et al., 2014). In general inhibitors are used in these procedures to control the metal dissolutions. Hydrochloric acid is extensively used in the preserving of steel and different alloys. Most popular inhibitors are organic compound containing N, S, and O atoms. Organic compound containing functional electronegative groups and π electrons in triple or conjugated double bonds are usually good inhibitors (Rochdi et al., 2014; Sastri et al., 1998; Lagrenée et al., 2002; Florio et al., 2004; Zarrok et al., 2012). These organic inhibitors are usually adsorbed on the metal surface via formation of a coordinate covalent bond (chemical adsorption) or the electrostatic interaction between the metal and inhibitor (physical adsorption) (Traisnel et al., 2013; Goulart et al., 2013).

In this work, the corrosion inhibition efficiency of three novel organic compounds (El Ghozlani et al., 2016), 6-Methyl-3-[1-(2-methyl-2H-indazol-6-ylamino)-ethylidene]-pyran-2,4-dione (R1), 3-[1-(2-Allyl-2H-indazol-6-ylamino)-ethylidene]-6-methyl-pyran-2,4-dione (R2),

* Corresponding author
E-mail addresses: m.elidrissi2018@gmail.com (M. El idrissi)

6-(2,5-Dimethyl-pyrrol-1-yl)-2-ethyl-2H-indazole (R3) (Figure 1) on mild steel in 1M hydrochloric acid solution was studied using potentiodynamic polarization curves, electrochemical impedance spectroscopy (EIS) and atomic force microscope AFM. Effects of inhibitors concentration and temperature on inhibition action were investigated.

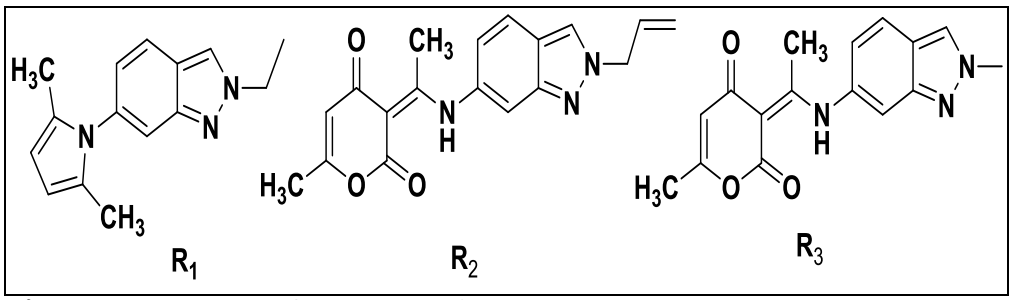

Fig. 1. Structures of R1, R2 and R3

2. Results

Theoretical computation

Computational method

DFT calculationwere carried out using the B3LYP functional (Yanai et al., 2004), together with the standard 6-31(d) basis set (Francl et al., 1982). The optimizations have been realized using the Berny analytical gradient. All computations have been shown with the Gaussian 09 suite of programs (Frisch et al., 1982). The global electrophilicity index (Liu et al., 1999) ω, μ and η, were given by the following expressions $\omega = \frac{\mu^2}{2\eta}$, $\mu = \frac{\varepsilon_H + \varepsilon_L}{2}$ and $\eta = \varepsilon_L - \varepsilon_H$, in terms of the electronic chemical potential μ and the chemical hardness η. Both quantities could be approached in terms of the one-electron energies of the frontier molecular orbital HOMO and LUMO, ε_H and ε_L, respectively.

Conceptual DFT essentially relies on the fact that the ground state energy of an N-electron system as given by the Hohenberg-Kohn theorem can be considered as depending upon the number of electrons N and the external potential v(r), which are themselves determined solely by the density, in other words $E[\rho_{(r)}]$ = E[N;v(r)]. In this context, the responses of the system to changes of the number of its electrons, of the external potential or of both, provide information about its reactivity.

The E[N ;v(r)] derivatives with respect to N and v(r) constitute a first series of reactivity indicators, the electronic chemical potential μ, which is the opposite of the electronegativity χ, the chemical hardness , the Parr function P(r) and the two variables linear response function χ (r,r'), as shown in the diagram given in (Figure 2).

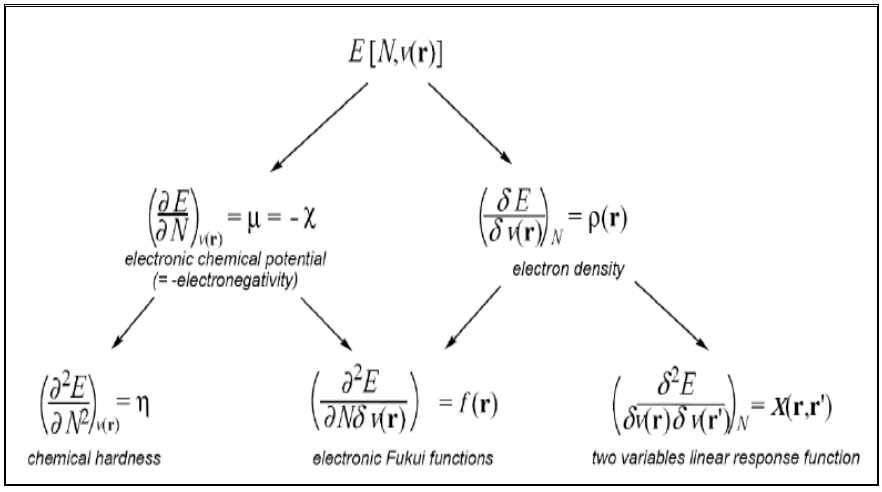

Fig. 2. First and second derivatives of E[N;v(r)] with respect to N and v(r)

Analysis of DFT reactivity indices of the reactants R1, R2 and R3

Quantum chemical calculations were conducted to understand the mechanism of inhibition of R1, R2 and R3 for mild steel in 303 K corrosion media. In particular, optimized geometric structures, electrostatic surface potential and frontier molecular orbital of R1, R2 and R3, including HOMO and LUMO electron density distributions for R1, R2 and R3 have been shown as (Figure 3). Then, the other parameters relating to quantum chemical calculation have been shown in (Table 1).

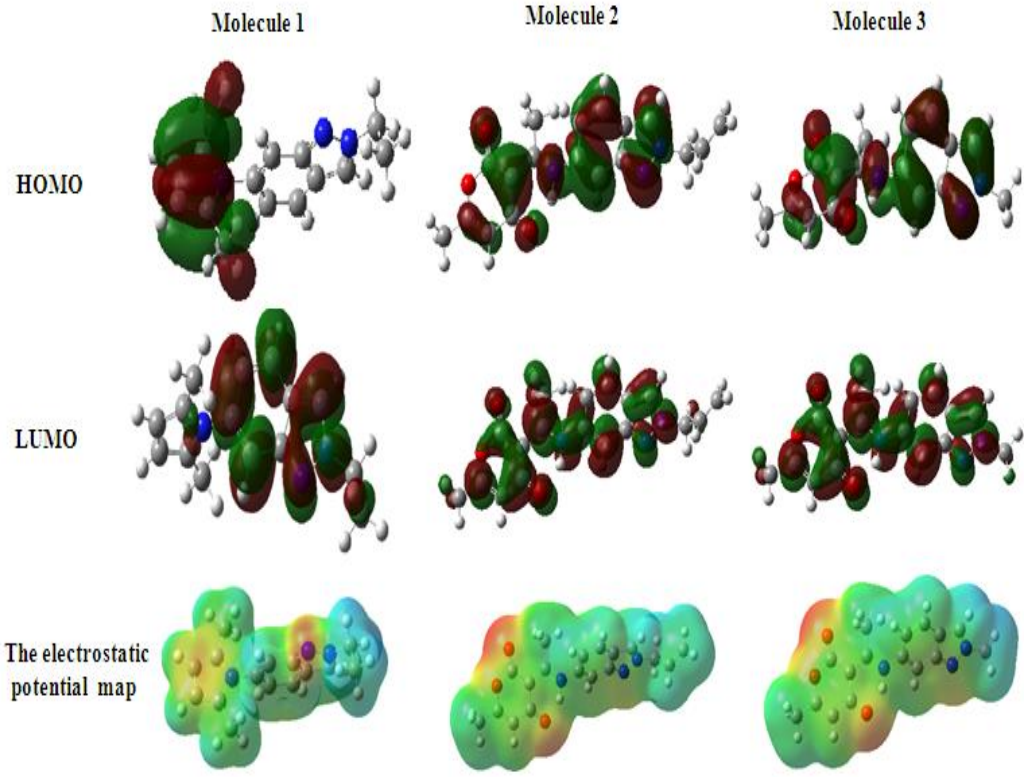

Fig.3. 3D representations of the frontier molecular orbital HOMO, LUMO and the electrostatic potential map of the three molecules

Table 1. Quantum chemical parameters for R1, R2 and R3 obtained in gaseous phase using the DFT at the B3LYP/6-31G level

Parameter	R1	R2	R3
EHOMO (eV)	-4.86374	-5.716277	-5.737774
ELUMO (eV)	-1.062396	-1.587062	-1.597403
Gap ΔE (eV)	3.801352	4.129215	4.140371
Dipole moment (μin Debye)	5.156800	5.694000	5.492600
Ionization potential (I in eV)	4.863748	5.716277	5.737774
Electron affinity (A)	1.062396	1.587062	1.597403
Electronegativity (χ)	2.963072	3.651669	3.667585
Hardness (η)	3.801352	4.129215	4.140371
Electrophilicity index (ω)	1.154825	1.614676	1.624396
Fractions of electron transferred (ΔN)	0.779478	0.884349	0.885811

The highest occupied molecular orbital value, E_{HOMO}, of the three inhibitors R1, R2 and R3 are, -4.863748, -5.716277 and -5.737774 respectively, show that the tendency of inhibitors R1 to donate electrons through to the acceptor molecule with an empty, the energy orbital. E_{LUMO} of the three inhibitors R1, R2 and R3 are -1.062396, -1.587062 and -1.597403 indicates the tendency of the molecule R1 to accept electrons.

The tendency being often that the lower E_{LUMO} is the largest; the ability of these molecules to accept electrons is greater. The energy gap ΔE is an important parameter related to the reactivity of

the inhibitor molecule about the metal surface. The energy gap ΔE of R1, R2 and R3 are, 3.801352, 4.129215 and 4.140371 respectively, a high ΔE of the inhibitor R2 and R3 are associated with a lower tendency to reactivity, whereas a weak ΔE of the molecule R1 indicates a strong tendency to reactivity.

We note from (Figure 4) that the HOMO orbital and the LUMO orbital of the R2 and R3 molecules are distributed on the indazole and pyrone groups, in contrary the molecule R1, the HOMO orbital is very localized on the pyrrole group and the LUMO orbital is very localize on the indazole group. The map of the electrostatic potential shows that the pyrone group of the inhibitors R2 and R3 has a red color, which shows that the pyrone group is very negative, conferring the great values of the dipolar moments of these molecules μ_2 = 5.694000 and μ_3 = 5.492600. On the contrary, in the molecule R1, the two pyrrole and indazole groups have a red color, which indicates that these two groups carry electrons, this distribution over the entire molecule abbesses the dipole moment of this molecule μ_1 = 5.156800.

Current studies indicate that the most favorable interaction is one that involves the interaction between the most electrophilic center of the electrophile and the most nucleophilic center of the nucleophile. Newly, Domingo (Domingo et al., 2016) exposeda new approach found on the electrophilic and nucleophilic Parr functions P_k^+ and P_k^-, respectively, which are found from the changes of spin electron-density take place from the nucleophile to the electrophile. This method demonstrates to be a dominant instrument for the study of the local reactivity. The maps of the ASD of these three inhibitors R1, R2 and R3 are given in (Figure 4).

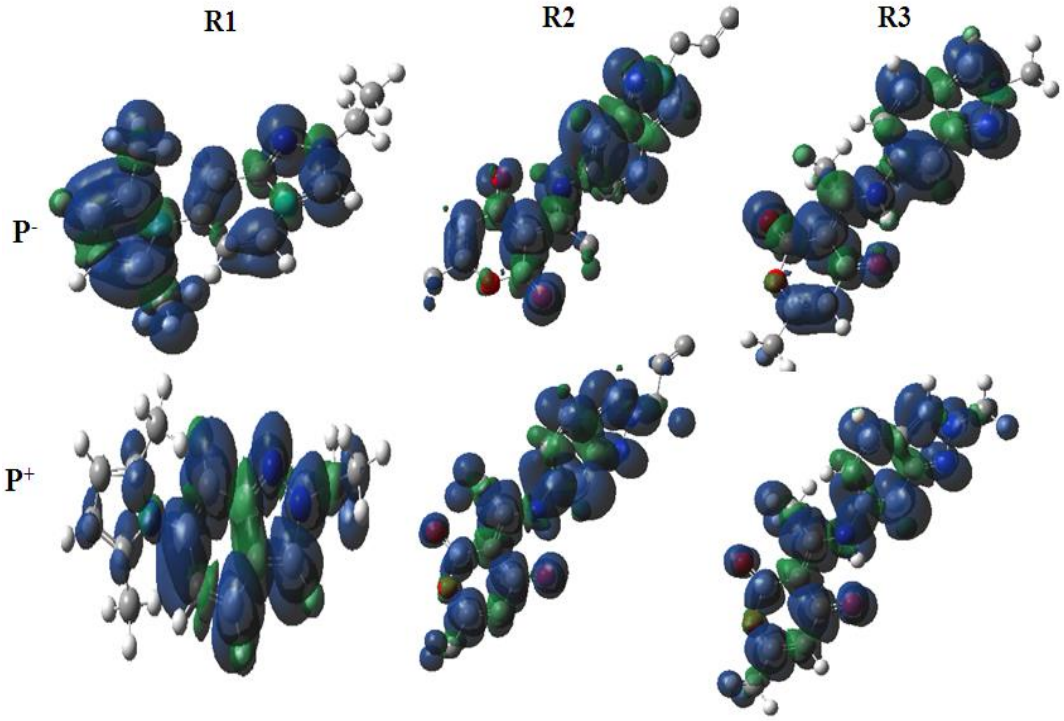

Fig. 4. The ASD of the radical anion and the radical cations as well as the electrophilic Parr functions and the nucleophilic Parr functions of the three inhibitors R1, R2 and R3

The Parr Functions P(r)

In case an amount equivalent to one electron is transferred, the nucleophile becomes a radical cation, while the electrophile becomes a radical anion. Interestingly, analysis of the atomic spin density (ASD) at the radical cation and the radical anion gives a picture of the distribution of the electron density in the electrophile and the nucleophile when they approach each other along the reaction progress.

Based on these observations, in 2014, Domingo proposed the Parr functions P(r) (Chamorro et al., 2013), which are given by the following equations:

$$P^-(r) = \rho_s^{rc}(r) \quad \text{For electrophilic attacks.}$$
$$P^-(r) = \rho_s^{ra}(r) \quad \text{For nucleophilic attacks}$$

Each ASD gathered at the different atoms of the cation and the radical anion of a molecule provides the local nucleophilic P_k^- and electrophilic P_k^+ Parr functions of the neutral molecule.

The values of nucleophilic Parr functions and the electrophilic Parr functions of these three inhibitors R1, R2 and R3 are given in (Table 2). (Numbering atoms in (Figure 5)).

Table 2. The values of the electrophilic Parr functions and the nucleophilic Parr functions of the three inhibitors R1, R2 and R3

Inhibitor R1			Inhibitor R2			Inhibitor R3		
	P^-	P^+		P^-	P^+		P^-	P^+
C1	0.384	0.014	C1	-0.052	0.030	C1	-0.053	0.031
C2	-0.013	0.009	C2	0.270	-0.080	C2	0.276	-0.084
C3	0.156	-0.003	C3	-0.034	0.094	C3	-0.035	0.098
C4	0.293	0.019	C4	0.039	-0.035	C4	0.040	-0.036
N5	-0.068	-0.011	C5	0.028	0.123	C5	0.028	0.129
C8	0.050	0.288	O7	-0.002	-0.009	O7	-0.002	0.001
C9	-0.020	-0.077	O8	0.032	0.068	O8	0.032	-0.010
C10	0.013	0.072	O9	0.129	0.021	O9	0.133	0.071
C11	-0.022	-0.072	C10	-0.001	-0.012	C10	-0.001	-0.012
C12	0.002	-0.011	C14	-0.094	0.306	C14	-0.096	0.316
C13	0.049	0.267	C15	0.006	-0.026	C15	0.006	-0.027
C14	0.079	0.175	N19	0.160	0.011	N19	0.163	0.015
N8	0.091	0.153	C21	0.239	0.200	C21	0.234	0.202
N19	-0.021	0.189	C22	-0.060	-0.043	C22	-0.057	-0.043
C20	0.001	-0.015	C23	0.023	0.033	C23	0.025	0.028
C27	-0.016	0.009	C24	-0.034	-0.012	C24	-0.033	-0.009
C31	-0.024	0.0008	C25	-0.017	-0.032	C25	-0.019	-0.029
			C26	0.087	0.103	C26	0.086	0.097
			C27	0.109	0.041	C27	0.106	0.033
			N31	0.220	0.082	N31	0.211	0.080
			N32	-0.024	0.087	N32	-0.021	0.088
			C34	0.0002	-0.010	C34	-0.0004	-0.009
			37C	-0.001	0.004			
			C38	0.002	0.0000			

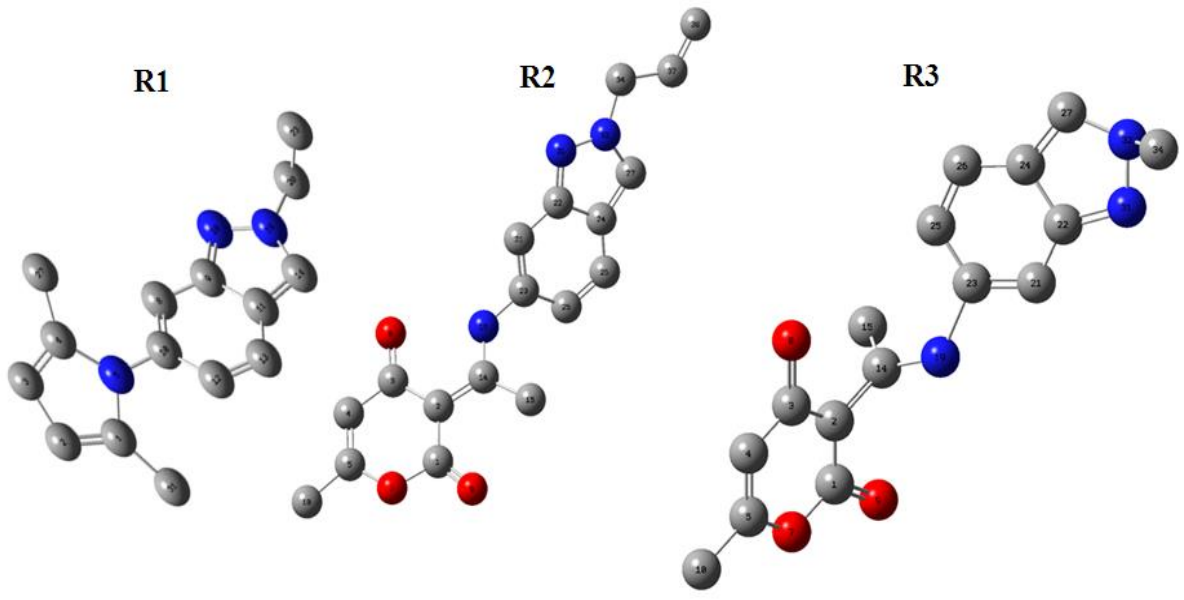

Fig. 5. Numbering atoms of the three inhibitors R1, R2 and R3

The computed values of the P_k^+ for the R1 inhibitor are mostly localized on the indazole ring (Table 2). Specifically the values of the centers C8, C13, C14, N8 and N19 are 0.288, 0.267, 0.175, 0.153 and 0.189 respectively, indicating that the these centers of the indazole ring are very favorite site for nucleophilic attack. The greatest values of the P_k^- for the R1 inhibitorare those carried by the atomsC1 (0.384), C3 (0.156) and C4 (0.293), indicating that these centers of the pyrrole ringare very favorite site for electrophilic attack.

The calculated nucleophilic Parr functions at the reactive sites of the R1 inhibitor, the C2, O9, N19, C21, C27 and N31 centers atoms are the most nucleophile site possessing a 0.270, 0.129, 0.160, 0.239, 0.109 and 0.220 respectively, indicates that totality of the global nucleophilicity of R1 inhibitor is accumulated at the these centers and these sites are very preferred for electrophilic attack. Similarly, the calculated electrophilic Parr functions at the reactive sites of R1 inhibitor reveal that the most electrophilic centers in this species are the C5, C14, C21 and C26 atoms possessing a P_k^+ value of 0.123, 0.306, 0.200 and 0.103 respectively, we can conclude that these centers are very favored for electrophilic attack.

The presence of the methyl group in the molecule 3 decreases the values of the Parr functions in the Indazole ring and increases the values of the functions on the 2-pyroneringand the values of the nucleophilic Parr functions grow to be C2 (0.276), O9(0.133), N19(0.163), C21(0.234), C27(0.106) and N31(0.211)and the electrophilic Parr functions become C5 (0.129), C14 (0.316), C21 (0.202) and C26 (0.097), The presence of the methyl groupin the molecule 3decreasesinhibition efficiency of this inhibitor.

3. Conclusion

Both R1 and R3 at a concentration more than 0.8 mM can effectively prevent corrosion of mild steel from the acidic medium. In comparison with R2, however, R1 and R3 exhibits higher inhibition efficiency in the concentration range of this study. Although the three compounds can both adsorb on metal surface through the electron donation or acceptance between the hetero-atoms and iron atoms.

4. Conflict of interests

The authors declare that there is no conflict of interests regarding the publication of this paper. Also, they declare that this paper or part of it has not been published elsewhere.

5. Acknowledgments

The authors are thankful for Laboratory of Chemical Process and Applied Materials. Sincere thanks are also due for Prof. Adil Belhaj, Department of Physique, Faculty of Science, Mohammed V University, Rabat, for valuable comments for the manuscript.

References

Chamorro et al., 2013 – *Chamorro, E., Pérez, P., Domingo, L.R.* (2013). On the nature of Parr functions to predict the most reactive sites along organic polar reactions. *Chem. Phys. Lett.* 582: 141-143.

Coughlin et al., 2004 – *Coughlin, R.* (2004). (2004). Corrosion inhibitors in: J.J. Florio, D.J. Miller (Eds.). Handbook of Coatings Additives, second ed., Marcel Dekker, New York, pp. 127-144.

Domingo et al., 2016 – *Domingo, L.R., Rios-Gutierrez, M., Emamian, S.* (2016). Understanding the stereoselectivity in Brønsted acidcatalysed Povarov reactions generating cis/trans CF3-substituted tetrahydroquinolines: a DFT study. *RSC Adv.* 6: 17064-17073.

El Ghozlani et al., 2016 – *El Ghozlani, M., Chicha, H., Abbassi, N., Chigr, M., El Ammari, L., Saadi, M., Spinelli, D., Rakib, E.M.* (2016). One-pot synthesis of new 6-pyrrolyl- N -alkyl-indazoles from reductive coupling of N -alkyl-6-nitroindazoles and 2,5-hexadione. *Tetrahedron Lett.,* 57: 113-117.

Francl et al., 1982 – *Francl, M.M., Pietro, W.J., Hehre, W.J., Binkley, J.S., Gordon, M.S., DeFree, D.J., Pople, J.A.* (1982). Self-Consistent Molecular Orbital Methods. XXIII. A Polarization-Type Basis Set for Second-Row Elements. *J. Chem. Phys.* 77: 3654-3665.

Frisch et al., 1982 – *Frisch, M.J.* (1982). Gaussian 09, Revision A.02.

Goulart et al., 2013 – *Goulart, C.M., Esteves-Souza, A., Martinez-Huitle, C.A., Rodrigues, C.J.F. Maciel, M.A.M., Echevarria, A.* (2013). Experimental and theoretical evaluation of semicarbazones and thiosemicarbazones as organic corrosion inhibitors. *Corros. Sci.* 67: 281-291.

Hamani et al., 2014 – *Hamani, H., Douadi, T., Al-Noaimi, M., Issaadi, S., Daoud, D., Chafaa, S.* (2014). Electrochemical and quantum chemical studies of some azomethine compounds as corrosion inhibitors for mild steel in 1M hydrochloric acid. *Corros. Sci.* 88: 234-245.

Lagrenée et al., 2002 – *Lagrenée, M., Mernari, B., Bouanis, M., Taisnel, M., Bentiss, F.* (2002). *Corros. Sci.* 44: 573-588.

Mourya et al., 2014 – *Mourya, P., Banerjee, S., Singh, M.M.* (2014). Corrosion inhibition of mild steel in acidic solution by Tageteserecta (Marigold flower) extract as a green inhibitor. *Corros. Sci.* 85: 352-363.

Parr et al., 1999 – *Parr, R.G., Szentpaly, L.V., Liu, S.* (1999). *J. Am. Chem. Soc.* 121: 1922-1924.

Rochdi et al., 2014 – *Rochdi, A., Kassou, O., Dkhireche, N., Touir, R., El Bakri, M., Ebn Touhami, M., Sfaira, M. Mernari, B. Hammouti, B.* (2014). Inhibitive properties of 2,5-bis (n-methylphenyl)-1,3,4-oxadiazole and biocide on corrosion, biocorrosion and scaling controls of brass in simulated cooling water. *Corros. Sci.* 80: 442-452.

Sastri et al., 1998 – *Sastri, V.S.* (1998). Corrosion Inhibitors-Principles and Applications. Wiley, Chichester, England.

Tourabi et al., 2013 – *Tourabi, M., Nohair, K., Traisnel, M. Jama, J. Bentiss, F.* (2013). Electrochemical and XPS studies of the corrosion inhibition of carbon steel in hydrochloric acid pickling solutions by 3, 5-bis (2-thienylmethyl)-4-amino-1, 2, 4-triazole. *Corros. Sci.* 75: 123-133.

van der Geer et al., 2010 – *van der Geer, J., Hanraads, J.A.J., Lupton, R.A.* (2010). The art of writing a scientific article. *J. Sci. Commun.* 163: 51-59.

Yanai et al., 2004 – *Yanai, T., Tew, D.P., Handy, N.C.* (2004). *Chemical Physics Letters.* 393: 51-57.

Zarrok et al., 2012 – *Zarrok, H., Zarrouk, A., Hammouti, B., Salghi, R., Jama, C., Bentiss, F.* (2012). Corrosion control of carbon steel in phosphoric acid by purpald–weight loss, electrochemical and XPS studies. *Corros. Sci.* 64: 243-252.